Discrepancy between repetition suppression and pattern analysis provides new insights into the role of M1 and parietal areas in sequence learning

Eva Berlot[1,*], Nicola J. Popp[1], Scott T. Grafton[2-3], & Jörn Diedrichsen[1,4,5,*]

[1] The Brain and Mind Institute, University of Western Ontario, Canada
[2] Department of Psychological and Brain Sciences, University of California, Santa Barbara, CA, USA
[3] Institute for Collaborative Biotechnologies, University of California, Santa Barbara, CA, USA
[4] Department of Statistical and Actuarial Sciences, University of Western Ontario, Canada
[5] Department of Computer Science, University of Western Ontario, Canada

Corresponding authors:
eva.berlot@gmail.com and jdiedric@uwo.ca

Abstract

How does the brain change during skill learning? We previously conducted a longitudinal fMRI motor sequence learning study and, using multivariate techniques, found learning-related changes in premotor and parietal areas, but not in the primary motor cortex (M1) (1). However, a study using repetition suppression (RS) had previously suggested that M1 represents learned sequences. Here we replicate this discrepancy in a single experiment, allowing us to investigate the differences between RS and multivariate pattern analysis in detail. We found that the RS effect in M1 and parietal areas reflect fundamentally different processes. M1's activity represents the starting finger of the sequence, an effect that vanishes with repetition. In contrast, activity patterns in parietal areas exhibit sequence dependency, which persists with repetition. These findings demonstrate that combining RS and pattern analysis can provide novel functional insights, here specifically into the relative contribution of cortical motor areas to sequence production.

Introduction

The ability to learn and produce complex sequences of movements is essential for many everyday activities, from tying laces to riding a bicycle and playing instruments. Searching for where these acquired skills are represented in the brain has been one of the central questions in motor neuroscience (2). One central issue in this debate is whether skilful sequence execution relies on representations in premotor and supplementary motor areas, or whether the sequences are represented in the primary motor cortex (M1) itself (3–11; for reviews see 12,13). We recently conducted a systematic longitudinal 5-week training study (1) employing functional magnetic resonance imaging (fMRI) to assess brain changes with motor learning. We observed no overall activity changes with learning in M1, and no changes in the sequence-specific activity patterns in this region. In contrast, clear learning-related changes in both overall activity and fine-grained activity patterns were observed in premotor and parietal areas, suggesting learning-related changes occur outside of M1. Other recent studies suggest that activity patterns in M1 reflect individual movement elements, but do not vary with the sequential context (9,11,14). This suggests that M1 does not represent learnt motor sequences, but must rely on inputs from other areas to initiate the next movement element.

Using the technique of repetition suppression, however, Wymbs and Grafton (15) provided evidence for skilled sequence representation in M1. Repetition suppression (RS) refers to the observation that a stimulus repetition evokes reduced neuronal activity compared to its initial presentation (16). This technique has been commonly used as a tool for investigating brain representation (17–24) following the logic that if, on average, regional activation reduces upon repetition, then the underlying neuronal population must represent at least one of the repeated aspects of the stimulus. Based on this, stronger RS effects are commonly interpreted as more robust representations (18). Wymbs and Grafton (15) found learning-related changes in RS across several regions,

including M1, suggesting that M1 might represent trained sequences. This stands in stark contrast to the above-mentioned studies that used pattern dissimilarity analyses and found no evidence of sequential representation in M1.

We reasoned that this discrepancy may reflect the fact that RS can be caused by a range of changes in the neuronal population code, and hence may reflect different changes in brain computation (18,25). To understand RS effects in more detail, we need to know what aspects of the underlying representations reduce from the first to the second repetition of a stimulus or movement. To address this question, we here performed a set of novel multivariate and RS analyses on the data from the longitudinal fMRI learning study (1). In the study, participants performed all sequences, trained and untrained, twice in a row, allowing us to conduct both pattern and RS analysis on the same data. We first replicate the discrepancy in the literature, with RS indicating that M1 develops a sequence representation with training, and multivariate analysis indicating the opposite. Using pattern analysis, we then decompose the activation patterns in the first and second repetition to determine which representational aspects underlie the RS effects in the different regions.

Results

Learning paradigm

We trained 26 participants to execute six 9-digit finger sequences with their right hand (**Fig 1a**), over a period of 5 weeks (**Fig 1b**). Participants also underwent scanning (using 7T MRI) while executing the 6 trained and 6 untrained sequences. In this paper we focus on results from week 1, i.e., before training, and week 5, i.e., after training (**Fig. 1c**; see **Methods** for details). The trials in the scanning sessions were structured so that the same sequence was always executed twice in a row (**Fig 1d**). This design choice

allowed us to contrast brain responses during the first execution to that of the second execution to examine repetition effects.

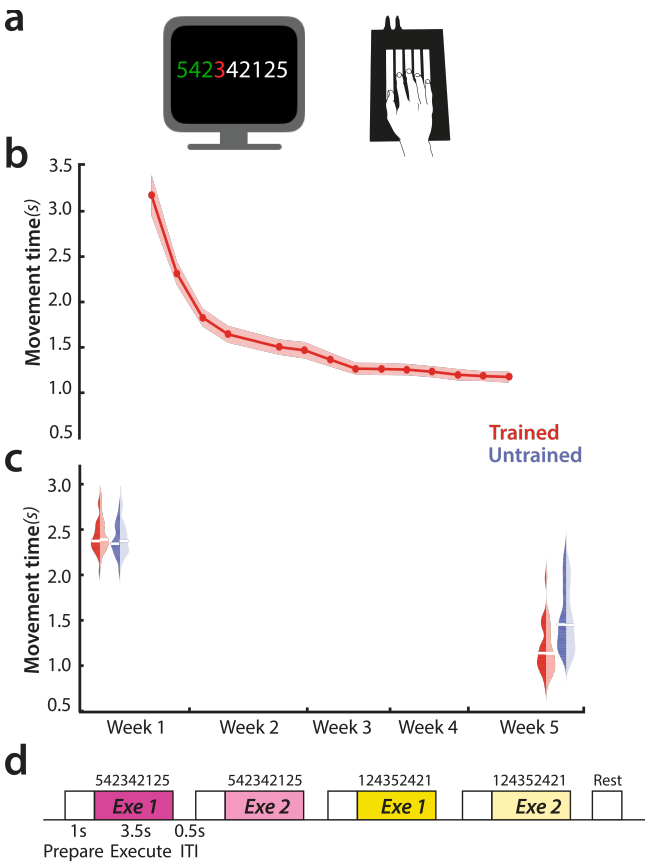

Figure 1. Experimental paradigm. a) Experimental setup – finger sequences composed of 9 digits were executed on a keyboard device. Participants received visual feedback on correctness of their presses – digits turned green for correct presses, red for incorrect presses. **b)** Group-averaged performance on trained sequences over the 5-week behavioural training protocol. Red shade indicates the standard error of the group mean. **c)** Group-averaged performance during the pre-training and post-training scanning sessions. Trained sequences are in red, untrained in blue. Dark colour indicates first execution, light second execution. White bars indicate the group mean performance. **d)** Experimental paradigm inside the scanner. Each sequence was presented twice in a row. Trials started with a 1s preparation time in which the 9-digit sequence was presented, followed by a 3.5s period of sequence execution and 0.5s of inter-trial interval (ITI). Periods of rest were intermixed between trials to allow for an estimate of resting baseline activation. Yellow and purple indicate two different motor sequences. Darker shades indicate first execution, lighter shades second execution.

Changes in repetition suppression and pattern dissimilarities with learning

To examine learning-related changes in repetition suppression and pattern analysis, we calculated both metrics on fMRI activation patterns in the pre-learning session (i.e. week 1), and in the post-learning session (week 5). Relative to rest, sequence execution activated the primary motor cortex (M1), the primary somatosensory cortex (S1), premotor dorsal and ventral regions, supplementary motor cortex and the superior parietal lobules (SPL; **Fig 2a-b**). Activity was higher for the first than for the second execution. The amount of repetition suppression was calculated as the difference in the elicited activation between the two executions of the same sequence (exe 2 – exe 1). Negative values indicate a relative reduction in activation with repetition, i.e., repetition suppression (RS). Already in week 1, prior to learning, RS was observed in nearly all regions displaying task-evoked activation (**Fig 2b-c**). In regions that showed de-activation during task performance (blue shades in **Fig 2a**), we observed positive difference values between the executions (areas in red shades in **Fig 2c**). This indicates that, both the amount of activation, as well as the amount of deactivation reduced with repetition.

Next, we examined whether the regions that exhibited RS also displayed distinct activity patterns for different sequences (i.e., sequence-specific representations). Pattern dissimilarities were calculated as the average crossvalidated Mahalanobis dissimilarity (i.e., Crossnobis dissimilarity) between activation patterns of all possible sequence pairs (see **Methods** for details). Overall, regions with dissimilar activity patterns for the different sequences corresponded to regions which also exhibited RS effects (**Fig 2c-e**). Additionally, both metrics (RS and pattern dissimilarities) increased with from week 1 to week 5, with the effect particularly pronounced in the parietal cortex (**Fig 2c, e**). Thus, based on visual inspection, RS and pattern dissimilarity metrics seem to provide consistent evidence for the development of sequence-specific representations with learning in an overlapping set of regions.

However, a more detailed inspection reveals some important differences between these two metrics. To show this, we focussed on a set of predefined regions of interest: the anterior SPL (SPLa), the dorsal premotor cortex (PMd), and M1. In SPLa and PMd, pattern dissimilarities increased specifically for the trained sequences (**Fig 2g**), as quantified by a significant interaction in a week x sequence type ANOVA (SPLa: $F_{(1,25)}$=4.80; p=.038, PMd: $F_{(1,25)}$=5.29, p=.030). The RS effects in the same regions paralleled those of pattern dissimilarities, with bigger increase in RS for trained than untrained sequences (**Fig 2f**; SPLa: $F_{(1,25)}$=17.44; p=3.1e^{-4}, PMd: $F_{(1,25)}$=7.27, p=1.1e^{-6}). Furthermore, the observed change in RS across weeks replicated a previously reported finding (15; see Figure 2–figure supplement 1). Thus, in PMd and SPLa, trained sequences exhibited more dissimilar activity patterns and a stronger RS, together suggesting these regions develop a dedicated representation of the trained sequences with learning.

In contrast, the two metrics diverged in M1. Here, pattern dissimilarities did not change with learning, i.e., the week by sequence type interaction was not significant (**Fig 2g**; $F_{(1,25)}$=2.13, p=.16). In contrast, RS increased more for trained than untrained sequences with learning (**Fig 2f**; $F_{(1,25)}$=25.09; p=3.6e^{-4}). These results, thus, replicate the previously reported discrepancy in findings showing increased RS in M1 with learning (15), yet no change in pattern dissimilarities (1), within the same dataset.

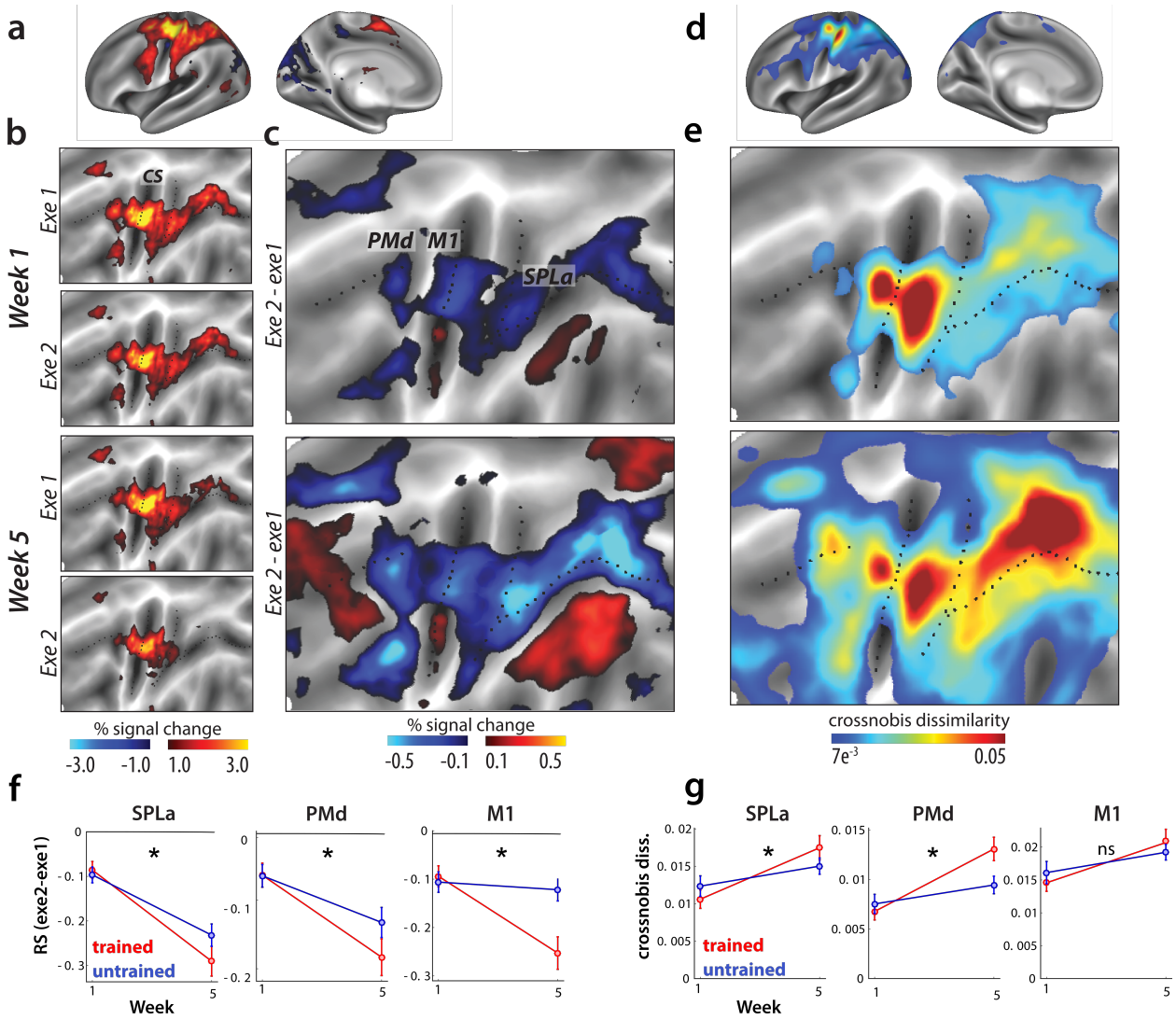

Figure 2. Changes in repetition suppression and dissimilarities with learning. a) Group-averaged evoked activation, measured as percent signal change over resting baseline in week 1, averaged across all sequences and projected to an inflated representation of the left hemisphere. **b)** Group-averaged activation for each execution (Exe1, Exe2), in the baseline session (Week 1) and after training (Week 5) represented on a flattened representation of the left hemisphere. CS stands for the central sulcus. **c)** The difference in evoked activation between the two executions. Blue represents relative suppression of activation on the second, relative to the first, execution. Regions of interest: primary motor cortex (M1), dorsal premotor cortex (PMd), anterior superior parietal lobule (SPLa). **d)** Average dissimilarity between evoked patterns for all pairs of sequences, in week 1, averaged across the group. Pattern dissimilarity was computed using a searchlight approach, by calculating the average Crossnobis dissimilarity of activation patterns between all sequence pairs in each searchlight. The mean dissimilarity of a searchlight

was assigned to its centre (see **Methods**). **e)** Average dissimilarity between activation patterns of different sequence pairs in weeks 1 and 4. **f)** Repetition suppression in the predefined regions of interest. Repetition suppression is calculated as the difference in group-averaged activation between the two executions for trained (red) and untrained (blue) sequences. Error bars reflect the standard error of the group. More negative values indicate more suppression during second execution, relative to the first. * signals $p<.05$. **g)** Dissimilarities between trained (red) and untrained (blue) sequence patterns, across weeks 1 and 5. Error bars reflect the standard error of the group. * signals $p<.05$.

Pattern dissimilarities reduce with repetition

Pattern analysis and RS therefore provide conflicting evidence on the nature of learning-related change in M1. While the increase in pattern dissimilarities (**Fig 2f**), as well as direct evidence for cross-session pattern changes (1), clearly argue that sequence-specific learning occurs in premotor and parietal areas and not in M1, RS provides evidence for the development of sequence-specific representations in both parietal / premotor regions and M1.

How can this discrepancy be explained? To resolve this question, we need to understand how the representations in each area during skilled performance change from the first to the second execution. We first inspected pattern dissimilarities for each of the two executions separately (execution 1, execution 2) in the trained state (Week 5). We observed that, on average, pattern dissimilarities in week 5 decreased with repetition in most cortical regions (**Fig 3a**). This decrease was particularly pronounced in M1 (**Fig 3b**).

The relationship between the reduction in overall activity with repetition and the reduction of pattern dissimilarity provides a way of distinguishing three different accounts of RS (**Fig 3c**; 18). According to one hypothesis (the scaling account), all of the involved voxels scale their activation with repetition, proportional to the initial activity in the first instance. This account predicts that dissimilarities reduce proportionally, i.e.

192 scale, to the decrease in activation. Alternatively (following the sharpening account),
193 representation could sharpen with repetition – this would occur if the neuronal population
194 most sensitive to different motor sequences would still be active on repetition, but the
195 less selective neurons (i.e., background noise) would decrease their activation. As a
196 third option (the fatigue account), the most active and selective neurons would decrease
197 their firing the most on repetition, resulting in a representational fatigue, which predicts
198 that dissimilarities reduce more than the reduction in overall activity.

199 Given this set of competing accounts, we first investigated how overall
200 dissimilarities within a region change across the two executions relative to changes in
201 activation within the same region. We quantified the amount of activation as the length
202 of the average activity vector relative to rest, separately for each execution (length of
203 lines in **Fig 3c**, see **Methods** for details). We then calculated the ratio of the activity
204 during the second execution over the activity during the first. This ratio was applied to
205 the observed dissimilarities on the first execution (dashed line in **Fig 3d**), yielding a
206 prediction of what dissimilarities would be expected for the second execution, if
207 representation scaled with activation. Relative to this expected dissimilarity, the
208 observed dissimilarities of M1 patterns were significantly lower during the second
209 execution (**Fig 3d**; $t_{(25)}$=3.87, p=6.9e^{-4}). This indicates that M1's representational change
210 is more in line with the representational fatigue account, which proposes that the
211 neuronal populations most tuned to performed sequences on the first execution reduce
212 their firing the most with repetition.

213 In contrast to M1, PMd and SPLa's dissimilarities on the second execution were
214 closer to the expected dissimilarities under scaling (**Fig 3e**; also see figure 3-figure
215 supplement 1 for a depiction of distance deviation from scaling across the cortical
216 sheet). To quantify whether the representational nature of repetition differed qualitatively
217 across regions, we performed a region x sequence type ANOVA. The main effect of

region was significant ($F_{(2,50)}$=7.42, p=1.5e^{-3}). Post-hoc t-tests revealed that this was driven by a significantly larger deviation from scaling in M1 as compared to SPLa ($t_{(25)}$=3.55, p=1.56e^{-3}). M1 and PMd did not differ from one another ($t_{(25)}$=1.25, p=.22). There was a significant difference between PMd and SPLa ($t_{(25)}$=2.65, p=.013), indicating a more 'scaling-like' representation in SPLa. There was no main effect of sequence type ($F_{(1,25)}$=1.35, p=.26), nor a region x sequence type interaction ($F_{(2,50)}$=2.10, p=.14). Altogether this indicates that representational change with repetition differed across regions: proportional scaling of representation in parietal regions, and much more pronounced decrease of dissimilarities in M1, similar to the fatigue account.

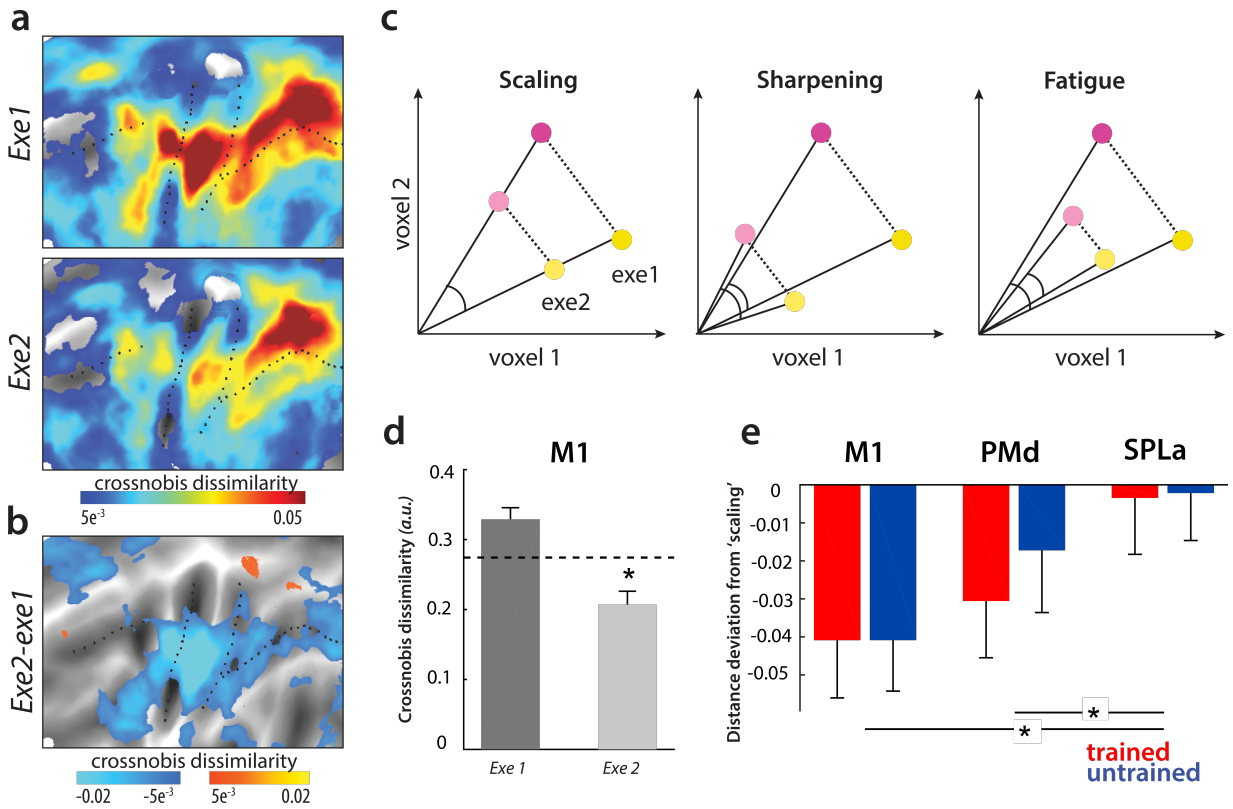

Figure 3. Representational change with repetition related to different hypothesized accounts of repetition suppression. a) Dissimilarities between pairs of sequences in week 5 (post-training), split by first and second executions. **b)** Difference in pattern dissimilarities between executions 1 and 2. Blue hues reflect relatively lower dissimilarities on the second execution. **c)** Different possible accounts of representational change with repetition. Yellow and purple indicate two different conditions, i.e. motor sequences in our paradigm. Darker shades

indicate first execution, lighter shades second execution. ***Scaling***: dissimilarities scale proportionally to activation reduction with repetition. ***Sharpening***: dissimilarities on the second execution are relatively higher than during the first execution, after accounting for activation reduction. ***Fatigue***: Dissimilarities reduce on repetition more than expected from the reduction in activation. **d)** Average Crossnobis dissimilarity between pairs of evoked sequence-specific patterns in week 5 in the primary motor cortex (M1), split by execution. Dashed line depicts expected dissimilarities if distances scaled proportionally with reduction of activation on repetition. The difference between dissimilarities on execution 2 and dashed line is plotted in e). * denotes $p<.05$ for comparison between the observed dissimilarities on execution 2 and the expected ones under scaling. **e)** Difference between the expected dissimilarity under scaling of activation and the observed dissimilarities on the second for trained (red) and untrained (blue) activity patterns. Regions: M1, dorsal premotor cortex (PMd), anterior superior parietal lobule (SPLa). Zero indicates proportional scaling with activation. * denotes $p<.05$.

Decomposing representations across executions 1 and 2

Analysis of average dissimilarities across executions revealed bigger compression of representation in M1 than in parietal regions. This analysis, however, does not reveal which aspects of the representations are responsible for this regional difference. To investigate exactly how the representation changed, we decomposed the representations during each execution into several underlying representational components. Differences in activity patterns can reflect differences in various characteristics, or features, of the performed sequences (**Fig 4a**). Specifically, based on previous results (11,14), we hypothesized that the covariance (or similarity) between activity patterns can be explained with the following 5 components (**Fig 4b**, see **Methods** for details): *1) first finger:* the pattern is determined by the starting finger, *2) all fingers*: the pattern reflects a linear mixture of finger-specific patterns, *3) sequence type*: trained and untrained sequences have different average patterns, *4) trained sequence identity*: the trained sequences differ amongst each other, *5) untrained sequence identity*: the untrained sequences (7-12) differ amongst each other. Using pattern component modelling framework (26), we constructed a model family out of these components,

which consisted of all possible combinations of those 5 components, totalling 2^5 models (see Figure 4-figure supplement 1a). These models were then fit to the observed regional covariance structure (second moment matrices; **Fig 4c**), separately for executions 1 and 2. The crossvalidated log Bayes factor relative to null model (i.e. no component present), and relative to the noise ceiling, is shown in Figure 4-figure supplement 1 for each of the combination models. To integrate the results across models, we then used Bayesian model averaging and estimated how much pattern variance was accounted for by each of these components (see **Methods** for details).

In M1, the regional representation on the first execution was accounted for by the individual movement elements (fingers), with especially high weight on the first finger (**Fig 4d**). This replicates the recent finding that M1's representation during sequence production tasks can be fully explained by the starting finger, but does not reflect differences later in the sequence (11,14). In the current study, we did not match the sequences in terms of the number of times each of the five fingers was pressed. Thus, subsequent finger presses, encoded in the 'all finger' component, also accounted for substantial variance, independent of the exact ordering of these movements.

To statistically quantify these effects, we calculated component Bayes factors for individual components. The Bayes factors were significant for both first and all finger factors (first finger: BF=13.3, $t_{(25)}$=3.1, p=4.8e^{-3}; all fingers: BF=19.6, $t_{(25)}$=4.1, p=3.4e^{-4}). In contrast, the component Bayes factors were not significant for any sequence-related feature – neither sequence type (BF=3.2, t=1.9, p=.07), nor sequence identity: of trained sequences (BF=1.6, $t_{(25)}$=1.5, p=.16) or untrained sequences (BF=0, $t_{(25)}$=-0.2, p=.85). Thus, the pattern analysis clearly shows that activity patterns during the first execution in M1 can be explained by a superposition of individual movements, without clear evidence of a sequence representation.

In SPLa and PMd, the variance explained during the first execution was well accounted for by sequence type (SPLa: BF=48.0, $t_{(25)}$=5.85, p=4.22e^{-6}, PMd: BF=55.2, $t_{(25)}$=4.97, p=4.0e^{-4}), and trained sequence identity (SPLa: BF=7.2, $t_{(25)}$=3.03, p=5.6e^{-3}; PMd: BF=6.0, $t_{(25)}$=2.5, p=.019). There was no significant evidence for representation of untrained sequence identity in either of the regions (SPLa: BF=0.8, PMd: BF=0; $t_{(25)}$<=1.1, p>=.28). In comparison to M1, the variance related on individual movements – either the first finger or all fingers were weaker across PMd and M1. In PMd the first finger still accounted for some variance (BF=4.1), but this was further reduced in SPLa (BF=0.5).

With repetition, the pattern component related to the first finger drastically reduced, in M1 by 93% (**Fig 4d**). The reduction in variance explained by the first finger component was larger than for the all finger component, which reduced by 75% (paired t-test: $t_{(25)}$=9.03, p=2.4e^{-9}). This indicates that the drastic reduction of average dissimilarities in M1 with repetition is mostly due a pronounced first-finger effect during the first execution that almost vanishes on the second execution. Large reductions in first finger effect were also observed in PMd (by 81%) and SPLa (by 83%). In contrast, the representation of sequence type and trained sequence identity in these areas clearly reduced less (PMd: sequence type: 44%, trained sequence: 64%; SPLa: sequence type: 49%, trained sequence: 55%). The statistical significance of these effects was confirmed using a paired t-test, comparing the % reduction of the first finger and trained sequence factors within each region (PMd: $t_{(25)}$=7.96, p=2.6^{-8}; SPLa: $t_{(25)}$=12.8, p=1.7e^{-12}).

In summary, SPLa's regional activation patterns were better accounted for by components related to the sequence identity than to the first finger, which also reduced much less with repetition. This likely explains why the average dissimilarities did not compress with repetition in SPLa regions as much as in M1. PMd's representation was in-between those of M1 and SPLa – more variance was accounted for by the first finger than in SPLa, but less than in M1. With repetition, the proportion of different components

to overall regional representation remained relatively stable in PMd and SPLa (**Fig 4e**), but changed substantially in M1 in that the dominant first-finger representation on the first execution nearly disappeared on the second execution.

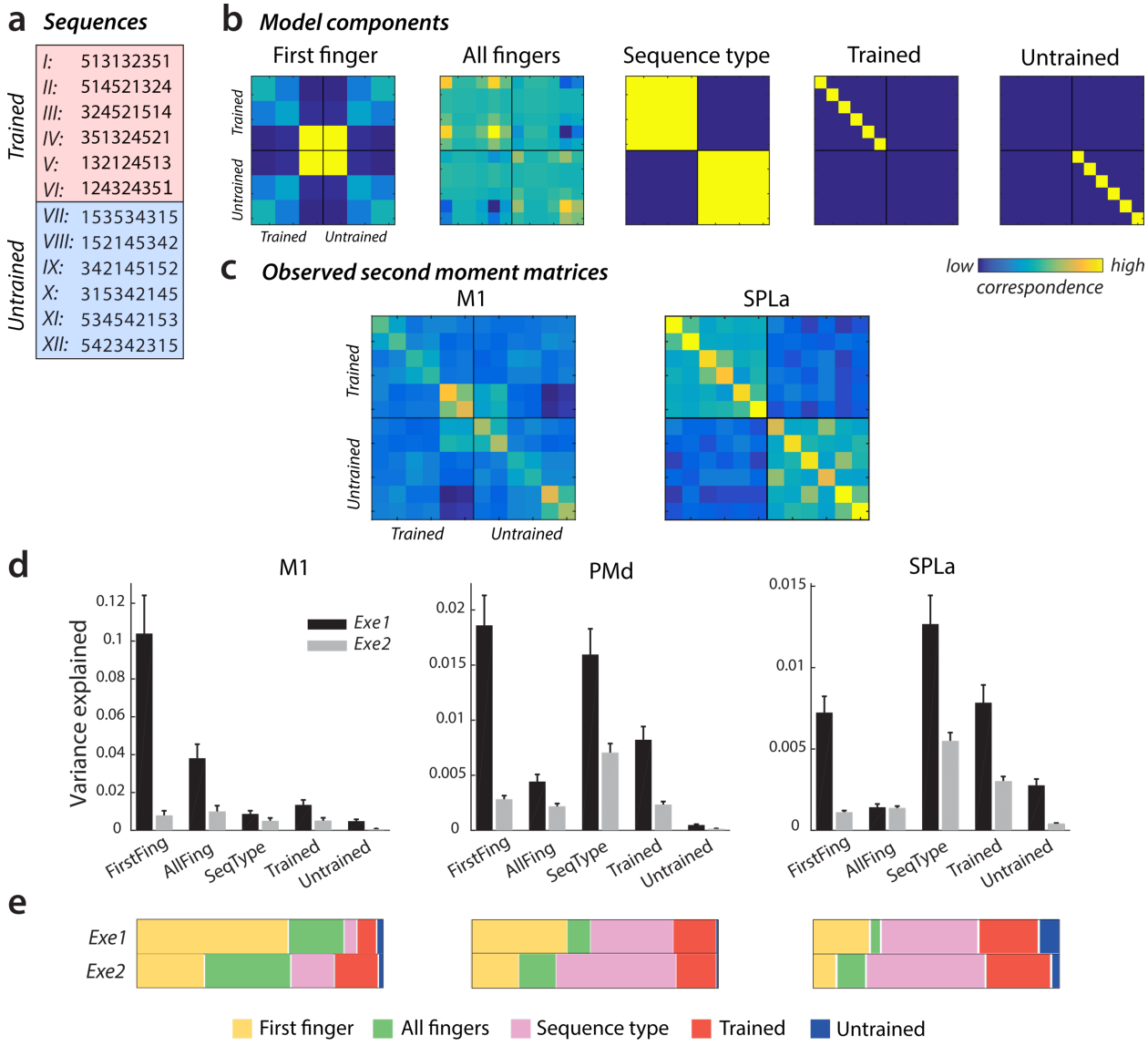

Figure 4. Component decomposition of regional representation across executions 1 and 2. a) Executed 9-digit sequences. Trained sequences of group 1 (presented here) were untrained for group 2, and vice versa. **b)** Candidate component models used to assess regional representations across first and second executions. Each row and column indicate a specific sequence, and values in the matrices reflect the correspondence across sequences on that component, with yellow indicating higher correspondence. **c)** Regional representations during the first execution of sequences, as assessed by the crossvalidated second moment matrix,

averaged across subjects of group 1. Similar as for models, each row and column reflect an activation pattern for an individual sequence. Regions: primary motor cortex (M1) and anterior superior parietal lobule (SPLa). **d)** Variance explained by candidate model components on executions 1 (black) and 2 (grey) in M1, PMd (dorsal premotor cortex) and SPLa. See figure supplement for performance of all models in model family. **e)** Relative contribution of variance explained in d) across the different components. The total variance explained across the different components (i.e. sum of the bars in d) was normalized across the two executions to display the relative shift of importance of different representational components.

Discussion

In the present study, we examined how brain representations of motor sequences evolve with training using a combination of pattern analysis and repetition suppression. Both pattern analysis and RS are commonly used to examine brain representations (18,27–30). The two methods often provide convergent results about the representational content of brain regions (18,24) – but sometimes there are discrepancies between the two. Specifically, in the context of motor sequence learning, previous studies using pattern analysis have reported no evidence of M1 representing trained motor sequences with learning (1,10,11). In contrast, one study (15) has reported learning-related increases in RS even for M1, which suggests a representation of the trained sequences in this region.

We first replicated the discrepancy between these two metrics in M1 in the same experiment. Closer examination of this discrepancy revealed that, with repetition, pattern dissimilarities decreased, particularly in M1. When decomposing regional representations into different underlying components, we observed that M1 mainly represents the first finger in a sequence. This component diminishes dramatically on a repetition. In contrast, the representation of sequence type and identity, which accounted for most of the variance in premotor and parietal areas, remained more stable across the two executions. This suggests that RS acts differently on different

358 components of neuronal representations; thus it's interpretation also varies across
359 regions which differ in their regional code.

360 Our findings suggest a new model of the interaction between parietal/premotor
361 areas and M1 during the execution of skilled motor sequences. During the first
362 execution, premotor and parietal regions contain information about the specific
363 sequence that needs to be executed (**Fig 5**). Additionally, premotor regions also reflect
364 the starting finger of the sequence. These regions send signals to M1, pre-activating the
365 neural circuits for the movement of the first finger. This replicates a previous finding that
366 the difference between M1's activation patterns is explained by the starting finger, rather
367 than reflecting true sequence representation (11). The finding is also consistent with
368 results from neurophysiology (31) and magneto-encephalography (MEG; 32), showing
369 the first action in a sequence is most highly activated in premotor and motor areas during
370 the preparatory period. Since M1 does not contain representation of sequence identity,
371 continuous signals from higher-order regions provide it with the sequential context
372 needed throughout the sequence production (9,33).

373 Upon repetition of the same sequence, activation reduces across all regions (**Fig**
374 **5**). This effect is already present before training, but its strength increases with training.
375 The global reduction in activation likely indicates that the initial volley of inter-regional
376 communication is established the first time, and does not need to be re-initialised (18).
377 The analysis of the regional representations in terms of their components indicates that
378 this reduction is most pronounced in the pre-activation of the first finger. In contrast, the
379 information about sequence identity in premotor and parietal regions reduces only
380 moderately, but otherwise remains similar to the first execution. This suggests that the
381 sequence representation is always necessary for successfully guiding M1 through the
382 correct sequences of actions, whereas the first finger does not need to be pre-activated
383 for a successful second execution.

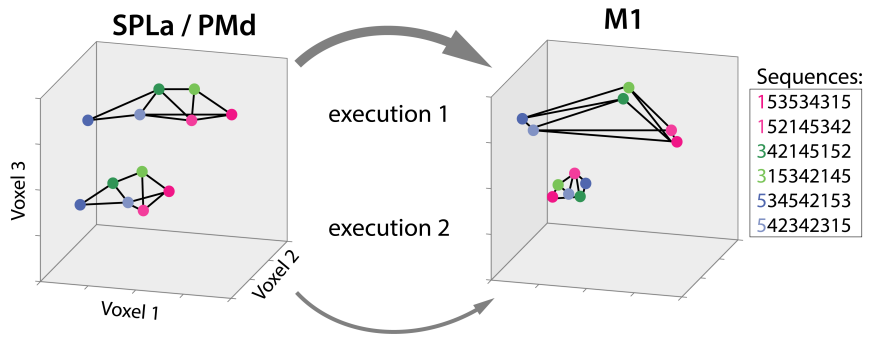

Figure 5. Conceptual depiction of changes in representation across regions and with repetition. Different dots represent activation patterns for different finger sequences. Regions: anterior superior parietal lobule (SPLa), dorsal premotor cortex (PMd), primary motor cortex (M1). Arrows depict communication between higher-order areas and M1. Activation levels of three hypothetical voxels are indicated across the 3 axes.

Overall, our results suggest that M1 does not represent individual trained sequences with learning, despite increased RS. Instead, its representation is characterized by combinations of finger presses. If this is true, why was RS in M1 stronger for trained than for untrained sequences? Since fMRI activation reflects the driving input into the area (34), this effect may reflect changes in the communication between higher-order areas and M1, which may become more efficient with repetition of trained sequences. Some support for this idea comes from a recent study demonstrating layer-specific effects in M1 (35). By measuring changes in cerebral blood volume across layers, the authors demonstrated that superficial M1 layers (which reflect inputs into M1) show RS, whereas deep layers' activation (which is more indicative of M1's outputs) is enhanced during repetition. Since the blood-oxygenated level depend signal (BOLD) is biased towards the superficial vascular signals, our activation results more likely reflect inputs into M1.

An alternative explanation for M1's increased RS for trained sequences is that M1 does contain sequence information, albeit at a spatial scale which cannot be detected

by pattern analyses. In line with this idea, a prior electrophysiology study reported differential M1's responses to trained relative to random sequences (8). This study, however, only reflected an overall difference between trained and random sequences, but not M1's differential activation for different trained sequences, thus no sequence representation as defined here. More recent electrophysiological studies have shown that M1 only represents the ongoing movement, and does not represent the sequential context (9,33). Altogether, this makes M1 representing individual trained sequences a less likely explanation of our results.

There are a number of limitations of the current study which merit future experimentation. First, our study did not differentiate between repetition suppression and expectation suppression (36,37). Expectation of repetition has been shown to modulate RS. We suspect that our observed effects would likely be weaker had the sequence repetition been less predictable, although we would not expect qualitatively different patterns of results. Second, the RS accounts tested here are by no means an exhaustive list. Other studies have examined additional models of RS (25,38). Some of those can only be tested with measurements providing better temporal resolution than that afforded by fMRI. For instance, a facilitation model predicts a faster start and finish of neuronal responses with repetition (22,39), which we are unable to assess using the sluggish temporal resolution of fMRI. Similarly, differences in neural synchronization across regions have been discussed as a mechanism of RS (40). MEG (41,42) or electrocorticography approaches (43) are more appropriate to test those accounts, and may provide important insights into the dynamics of parietal-premotor-M1 interactions.

Nevertheless, with the RS accounts employed here, we demonstrated that RS can reflect very different representational changes from the first to the second execution depending on the regions. During the repetition of skilled motor sequences, associative cortical regions represent the sequence itself in a stable fashion, while the activation in M1 changes qualitatively, with a reduced activation of the beginning of the sequence.

These results emphasize that employing RS only using the average regional activation sometimes provides incomplete, and possibly misleading, insights into regional representation. Instead, RS should be combined with pattern analyses to determine how the representations change with repetition, to ultimately provide a deeper understanding of brain circuits and their function.

Materials and Methods

Participants

Twenty-seven participants took part in the experiment. Data of one participant were excluded because their fieldmap was distorted in one of the four scans, resulting in 26 participants whose data was analysed (17 females, 9 males). Their mean age was 22.2 years (SD = 3.3 years). Criteria for study inclusion were right-handedness and no prior history of psychiatric or neurological disorders. They provided written informed consent to all procedures and data usage before the study started. The experimental procedures were approved by the Ethics Committee at Western University.

Apparatus

Finger sequences were performed using a right-hand MRI-compatible keyboard device (**Fig 1a**). The keys of the device had a groove for each fingertip, with keys numbered 1-5 for thumb-little finger. The keys were not depressible, so participants performed isometric finger presses. The force of the presses was measured by the force transducers underneath each finger groove (FSG-15N1A, Sensing and Control, Honeywell; dynamic range 0-25 N; update rate 2 ms; sampling 200 Hz). For the key to be recognized as pressed, the applied force had to exceed 1 N.

Learning paradigm

Participants were trained over a five-week time period to perform six 9-digit finger sequences. They were split into two groups, with trained sequences of one group being the untrained sequences of the second group, and vice versa (see **Fig 4b** for all of the chosen sequences). The chosen sequences for both groups were matched as closely as possible on several features: starting finger, number of repetitions per finger, and first-order finger transitions. The decision to split participants into two groups was made

466 to ensure that none of the observed effects could be due to the specific set of sequences
467 chosen.

468 On day 1 of the study, participants were acquainted with the apparatus and the
469 task performed in the scanner. To ensure no sequence-specific learning would take
470 place prior to scan 1, we used finger sequences different from the trained and untrained
471 sets which participants did not encounter at any later stage of the experiment.

472 During the behavioral training sessions, participants were trained to perform the
473 six sequences. Each training session was split into several blocks with 24 trials in each
474 block (i.e. 4 repetitions of each of the 6 sequences). Participants received visual
475 feedback on the correctness of their presses online with digits turning green for correct
476 presses and red for incorrect presses (**Fig 1a**). They were instructed to perform the
477 sequences as fast as possible, while keeping the overall accuracy within each block
478 <15% error rate. To encourage fast and accurate performance throughout the training,
479 participants received 0, 1 or 3 points after each trial completion based on correctness
480 and movement time (MT) – time from the first press until the last release in the sequence.
481 Specifically, they received 1 point for correct presses performed at their median MT, 3
482 points for correct presses executed at least 20% faster than their median speed until
483 that point. If they made a mistake on any of the presses or the MT in the trial was lower
484 than their median MT, they received 0 points. The median MT threshold was dynamically
485 adjusted across blocks every time a block was completed with an error rate <15% and
486 the median MT faster than previous threshold. Overall, their MT decreased across the
487 five weeks of training (**Fig 1b**).

488 We included several other design features in the behavioural training, such as
489 behavioural test sessions comparing participants' performance of trained sequences to
490 random sequences, and their performance using the left hand. Those sessions were not
491 assessed for this paper, and have been described elsewhere (1).
492

Experimental design during scanning

Participants underwent a total of 4 MRI scanning sessions (**Fig 1c**) while executing trained and untrained sequences. The first session served as a baseline prior to the start of the training protocol (in week 1), where the “trained” and “untrained” sequences were both untrained and seen for equivalent amount. The second session was conducted in week 2, and the last two after training protocol was completed – in week 5. In scanning sessions 1-3, participants’ performance inside the scanner was paced with a metronome, whereas in session 4, they performed as fast as possible. For the purpose of this paper, data of scanning session 1 (prior to training) and 4 (fully skilled performance) were analysed (**Fig 1c**). Session 4 allows for the closest comparison to the previous RS study (15) which also employed a full-speed performance design. Pattern analyses of sessions 2 and 3 are reported in (1).

Each scanning session consisted of eight functional runs with event-related design randomly intermixing trials containing the 6 trained and the 6 untrained sequences (totalling 72 trials per functional run). Each sequence was executed for two trials in a row (**Fig 1d**). The trial started with a 1 second preparation time with nine digits of the sequence presented on the screen. A ‘go’ signal was presented afterwards. In scans 1-3, a pink line appeared underneath the sequence and started expanding, indicating the pace at which participants were to press. In scan 4, participants executed the sequence as fast as possible after the go cue. After execution, they received feedback on their overall performance – 3 points for correct and 0 for incorrect performance. Each trial lasted for 5 s total (**Fig 1d**), with a 0.5 s inter-trial interval. Five periods of 10 s rests were added throughout each functional run to provide a better estimate of baseline activation. These rests were added randomly, but never between the first and second execution of the same sequence. In total, each scanning session lasted for approximately 75 minutes.

Image acquisition

Data were acquired on a 7-Tesla Siemens Magnetom MRI scanner with a 32-receive channel head coil (8-channel parallel transmit). At the beginning of the first scan, we acquired anatomical T1-weighted scan for each participant. This was obtained using a magnetization-prepared rapid gradient echo sequence (MPRAGE) with voxel size of 0.75x0.75x0.75 mm isotropic (field of view = 208 x 157 x 110 mm [A-P; R-L; F-H], encoding direction coronal). Data during functional runs were acquired using the following sequence parameters: GRAPPA 3, multi-band acceleration factor 2, repetition time [TR] = 1.0 s, echo time [TE] = 20 ms, flip angle [FA] = 30 deg, slice number: 44, voxel size: 2x2x2 mm isotropic. To estimate magnetic field inhomogeneities, we acquired a gradient echo field map with the following parameters: transversal orientation, field of view: 210 x 210 x 160 mm, 64 slices, 2.5 mm thickness, TR = 475 ms, TE = 4.08 ms, FA = 35 deg.

Preprocessing and first level analysis

Data preprocessing was carried out using SPM12 and custom MATLAB code. Preprocessing of functional data included correcting for geometric distortions using the acquired fieldmap data, and head motion correction (3 translations: x, y, z; 3 rotations: pitch, roll yaw). The data across sessions were all aligned to the first run of the first session, and then co-registered to the anatomical scan.

Preprocessed data were analysed using a general linear model (GLM; 44). We defined a regressor for each of the performed 12 sequences (6 trained, 6 untrained), separately for their first and second execution – resulting in a total of 24 regressors per run. The regressor was a boxcar function defined for each trial, and convolved with a two-gamma canonical hemodynamic response function (time to peak: 5.5 s, time to undershoot: 12.5 s). All instances of sequence execution were included into estimating

546 regressors, regardless of whether the execution was correct or erroneous. This analysis
547 choice was also taken by (15), thus allowing a more direct comparison of repetition
548 suppression results. Even when the error trials were excluded (i.e. removing all error
549 trials as well as second execution trials when the first execution was erroneous), our
550 results remained unchanged. Ultimately, the first level analysis resulted in activation
551 images (beta maps) for each of the 24 conditions per run, for each of the four scanning
552 sessions.
553

554 ## Surface reconstruction and regions of interest

555 Individual subject's cortical surfaces were reconstructed using FreeSurfer (45), and
556 aligned to the FreeSurfer's Left-Right symmetric template (Workbench's 164 nodes
557 template) via spherical registration. For our regions of interest (ROI), we defined areas
558 covering the primary motor cortex and secondary associative regions. The primary motor
559 cortex (M1) was defined using probabilistic cytoarchitectonic map (46) by including
560 nodes with the highest probability of belonging to Brodmann area (BA) 4 which in
561 addition corresponded to the hand knob area (47). The dorsal premotor cortex (PMd)
562 was included as the lateral part of the middle frontal gyrus. The anterior part of the
563 superior parietal lobule (SPLa) was defined to include anterior, medial and ventral
564 intraparietal sulcus.
565

566 ## Evoked activation and repetition suppression

567 We calculated the percent signal change for execution of each sequence relative to the
568 baseline activation for each voxel. The calculation was split between the first and second
569 execution. To calculate repetition suppression, the activation during the first execution
570 was subtracted from the elicited activation during the second execution. Thus, negative
571 values of this difference contrast represented relative suppression of activation on the
572 second execution, i.e. repetition suppression. For most subsequent analyses, the

obtained values of activation and repetition suppression were averaged separately for trained and the untrained sequences. For ROI analysis, the volume maps were averaged across the predefined regions (M1, PMd, SPLa) in the native volume space of each subject. Additionally, for visualization the volume maps were projected to the surface for each subject, and averaged across the group in Workbench space.

Dissimilarities between activity patterns for different sequences

To evaluate which regions displayed sequence-specific representation, we calculated Crossnobis dissimilarities between the evoked beta patterns of individual sequences. To do so, we first multivariately prewhitened the beta values – i.e. we standardized them by voxels' residuals and weighted by the voxel noise covariance matrix. Prewhitening has previously been found to increase the reliability of dissimilarity estimates (48). Next, we calculated the crossvalidated squared Mahalanobis dissimilarities (i.e. the Crossnobis dissimilarities) between evoked regional patterns of different pairs of sequences, resulting in a total of 66 dissimilarities. This was performed twice: once by combining the activation patterns across the two executions and second time by separately obtaining dissimilarities between evoked patterns split per execution. The obtained dissimilarities were then averaged overall, as well as separately within the pairs of trained sequences, and the untrained sequences.

The multivariate analysis was conducted separately for each ROI and then repeated using a surface searchlight approach (49). For each surface node, a circular region of 120 voxels was defined and Crossnobis dissimilarities were calculated amongst those voxels, with the resulting dissimilarities values assigned to the centre of the searchlight. The searchlight was then moved across the cortical sheet in a continuous manner.

Assessing accounts of repetition suppression

We examined several proposed accounts of RS – scaling, sharpening and fatigue (**Fig 3c**), by relating the observed changes in pattern dissimilarities with repetition to activation changes with repetition. Activation pattern for each sequence can be characterized as a point in a high-dimensional space, with each axis referring to the activation of a voxel. As a measure of the overall activation, we used the length of the activity vector from the origin (rest), and as dissimilarities the lengths of the vectors between different dots (**Fig 3c**). Unbiased estimates of the length of activity vectors relative to rest were derived from the crossvalidated second-moment matrix. The square root of each diagonal element (variance of evoked pattern) indicates the length of the activity vector, relative to rest. The square root of Crossnobis dissimilarity (variance – covariance between patterns) is the length of the vector between the two patterns (50). These measures were averaged across the 6 trained, and 6 untrained conditions, separately for executions 1 and 2.

For each subject and region, we then computed the decrease in activation as activity length for 2nd execution divided by activity length for the 1st execution. If dissimilarities decreased proportional to changes in activation, we would expect the ratio of dissimilarities between the two executions to equal the ratio obtained from activity vector lengths. Likewise, the dissimilarities expected under the scaling account can be computed as: $\mathrm{diss}_{\mathrm{scaling}} = \frac{\mathrm{act}_{\mathrm{exe2}}}{\mathrm{act}_{\mathrm{exe1}}} \mathrm{x}\, \mathrm{diss}_{\mathrm{exe1}}$. This expected dissimilarity value was compared to the observed dissimilarities on the second execution. Higher value of the observed relative to expected dissimilarity would be in line with the 'sharpening' account, lower value would be in support of the 'fatigue' account, while a value that wouldn't differ from the expected dissimilarities would support the 'scaling' account of RS for that region.

Pattern component analyses: modelling representational components

The analysis on dissimilarities between sequence-specific activity patterns is sensitive to any possible difference between patterns of different sequences. To decompose what specific features of stimuli might be driving these differences, we used pattern component modelling (PCM; 26,51). PCM models the covariance structure (second moment matrix) of regional activity patterns according to different representational hypotheses. In our experiment based on presented sequences, we defined five representational components.

1) First finger

Both trained and untrained sequences started with 3 possible fingers: thumb, middle finger and pinky finger. The first finger feature characterizes activity pattern as different for sequences starting with different first finger, and indistinguishable for sequences starting with the same first finger. The model component was weighted by the natural statistics of hand movement (52).

2) All fingers

The chosen sequences had slight differences in terms of how many times different fingers were executed in the sequence. Thus, the 'all fingers' feature characterized number of repetitions across fingers and how correspondent different sequences were in finger repetitions. Also this model component was weighted by the natural statistics of hand movement (52).

3) Sequence type

This component split the performed sequences based on whether they were trained or not, predicting different regional representations between trained and untrained sequences, but indistinguishable patterns within each of the two groups.

4) Trained sequence identity

This component assumes that each of the trained sequences is associated with unique activity patterns.

5) Untrained sequence identity

Similar as the trained sequence identity component, this component assumes unique activity patterns for different untrained sequences.

The overall predicted second moment matrix (G) was then a convex combination of the component matrices (G_c):

$$G = \sum_c \exp(\Theta_c)\, G_c$$

The construction of the models was split between the two groups of participants, as different sequences constituted 'trained' or 'untrained' sequences for the two groups. The subsequent steps of model fitting and evaluation were carried together for all subjects.

We formulated a family of models containing all possible combinations of the five chosen components. This resulted in 32 combinations (Figure 4-figure supplement 1), also containing the 'null' model without any component, which predicted no differences amongst any of the sequence patterns. We then evaluated all of the 32 models using a crossvalidated leave-one-subject-out scheme, estimating the likelihood of the observed regional second moment data under each model. The resultant cross-validated likelihoods were used as evidence of the model. The difference between the log-likelihood of each model and the null model results in a log-Bayes factor representing the relative model evidence over a null model.

In addition to the model family of the chosen components, we also fit a 'noise-ceiling' model to assess the maximal explainable information present in each region's representation across participants (26,53). For each of the two groups, we predicted the second moment matrix of a left-out subject based on n-1 subjects in the same group. This metric of inter-subject consistency was then combined across the subjects of the two groups.

To integrate the results across models, we used model averaging to determine the amount of pattern variance accounted for by each component in the context of all the other components. Prior to fitting, we normalized the trace of each model component to be 12 (number of conditions). Thus, the fitted component weight $\exp(\Theta_i)$ can be taken as the amount of variance accounted for by the component in the context of that model. Assuming a uniform prior probability across models, we compute a posterior probability of each model i (from 1 to 32) directly from their Bayes factors:

$$posterior_i = \frac{\exp(logBF_i)}{\sum_{j=1}^{c} \exp(logBF_j)}$$

The model-averaged amount of variance accounted for by each component c is then given by:

$$variance_c = \sum_{i=1}^{32} posterior_i \; x \; \exp(\Theta_c)$$

Important to note is that this variance calculation always results in positive estimates.

Data availability

The dataset used for these analyses is publicly available on OpenNeuro (doi: 10.18112/openneuro.ds002776.v1.0.2).

Acknowledgments

The work was supported by an Ontario Trillium Scholarship to EB, an NSERC Discovery Grant (RGPIN-2016-04890) to JD, and the Canada First Research Excellence Fund (BrainsCAN). We thank Giacomo Ariani for helpful comments on an earlier version of the manuscript.

Supplementary Figures

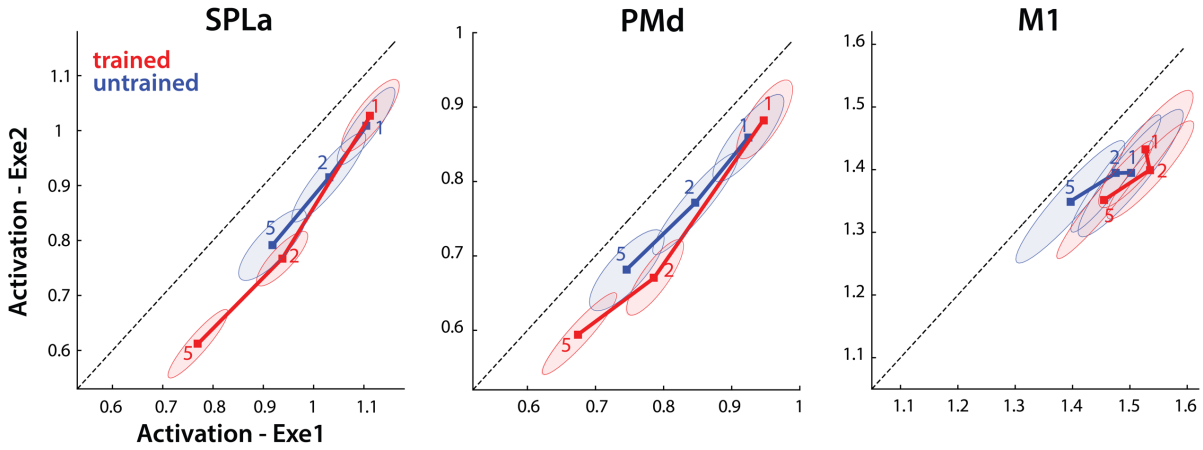

Figure 2-figure supplement 1. Learning-related changes in repetition suppression. Activation elicited on the first (x-axis) and second (y-axis) execution for trained (red) and untrained (blue) sequences across weeks 1, 2 and 5, in sessions using paced performance. Regions: anterior superior parietal lobule (SPLa), dorsal premotor cortex (PMd), primary motor cortex (M1). Ellipses reflect the standard error of the group. Dots below the diagonal line indicate activation was lower on second execution.

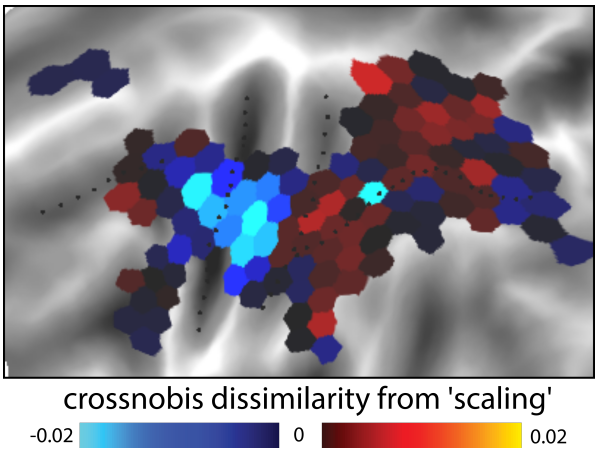

Figure 3-figure supplement 1. Difference in the Crossnobis dissimilarity on second execution from the 'scaling' account prediction. This was calculated for each of the regularly tessellated regions. Blue depicts lower dissimilarities than expected under the scaling account, yellow higher dissimilarities than predicted under scaling of activation.

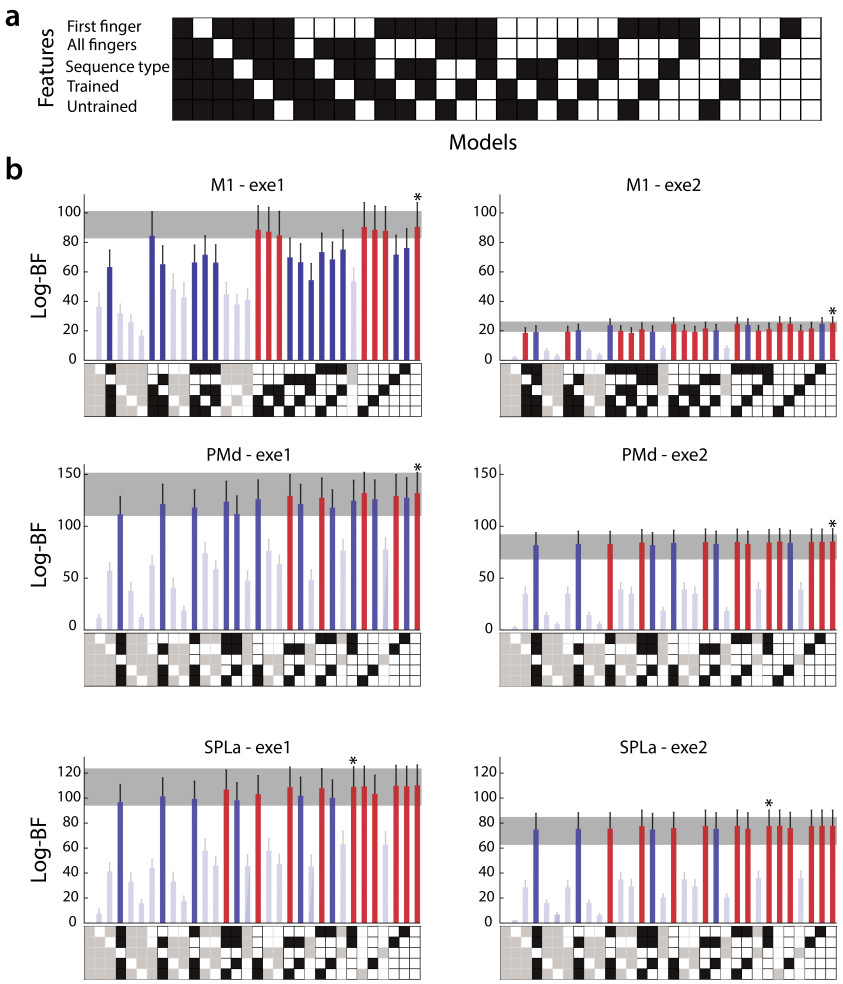

Figure 4-figure supplement 1. Pattern component modelling – formulation and model fits. **a)** Construction of a model family from the five components. All possible combinations of five components were used to construct models, resulting in 32 (2^5) models. The first model is a 'null' model (no component) and the last is a full model (all components). White squares indicate presence of the component in each model. **b)** Evidence for all models across regional activation, separately examined for the first and second sequence execution (left, right column). Regions: primary motor cortex (M1), dorsal premotor cortex (PMd), anterior superior parietal lobule (SPLa). The 32 evaluated models are presented on the x-axis. Model fits were assessed with a type-II log-likelihood. The difference in log-likelihood between each model and the null model was calculated; this can be interpreted as a log-Bayes factor (Log-BF) and is plotted on the y-axis. The grey shaded area represents the mean noise ceiling ± standard error of the group mean. The bar with a star is the best performing model. All models in red performed within the noise ceiling and did not differ from one another. Bars in dark blue depict models which hit the noise ceiling, but performed significantly worse than the best performing model. Bars in light blue did not reach the noise ceiling performance.

References

1. Berlot E, Popp NJ, Diedrichsen J. A critical re-evaluation of fMRI signatures of motor sequence learning. Elife. 2020;9(e55241):1–24.
2. Lashley K. In search of the engram. 1950.
3. Floyer-Lea A, Matthews PM. Distinguishable brain activation networks for short- and long-term motor skill learning. J Neurophysiol. 2005;94(1):512–8.
4. Karni A, Meyer G, Rey-Hipolito C, Jezzard P, Adams MM, Turner R, et al. The acquisition of skilled motor performance: fast and slow experience-driven changes in primary motor cortex. Proc Natl Acad Sci U S A. 1998;95(3):861–8. Available from: http://www.ncbi.nlm.nih.gov/pubmed/9448252%5Cnhttp://www.pubmedcentral.nih.gov/articlerender.fcgi?artid=PMC33809
5. Karni A, Meyer G, Jezzard P, Adams MM, Turner R, Ungerleider LG. Functional MRI evidence for adult motor cortex plasticity during motor skill learning. Nature. 1995;377(6545):155–8. Available from: http://www.nature.com/doifinder/10.1038/377155a0%5Cnhttp://www.ncbi.nlm.nih.gov/pubmed/7675082
6. Lehéricy S, Benali H, Van de Moortele P-F, Pélégrini-Issac M, Waechter T, Ugurbil K, et al. Distinct basal ganglia territories are engaged in early and advanced motor sequence learning. Proc Natl Acad Sci U S A. 2005;102(35):12566–71. Available from: http://www.pubmedcentral.nih.gov/articlerender.fcgi?artid=1194910&tool=pmcentrez&rendertype=abstract
7. Penhune VB, Doyon J. Dynamic cortical and subcortical networks in learning and delayed recall of timed motor sequences. J Neurosci. 2002;22(4):1397–406. Available from: http://www.ncbi.nlm.nih.gov/pubmed/11850466
8. Matsuzaka Y, Picard N, Strick PL, Barnes TD, Mao J, Hu D, et al. Skill Representation in the Primary Motor Cortex After Long-Term Practice Skill Representation in the Primary Motor Cortex After Long-Term Practice. J Neurophysiol. 2011;(December 2006):1819–32.
9. Russo AA, Khajeh R, Bittner SR, Perkins SM, Cunningham JP, Abbott LF, et al. Neural trajectories in the supplementary motor area and primary motor cortex exhibit distinct geometries, compatible with different classes of computation. Neuron. 2020;107(1–14).
10. Wiestler T, Diedrichsen J. Skill learning strengthens cortical representations of motor sequences. Elife. 2013;2013(2):1–20.
11. Yokoi A, Arbuckle SA, Diedrichsen J. The role of human primary motor cortex in the production of skilled finger sequences. J Neurosci. 2018;38(6):1430–42.
12. Dayan E, Cohen LG. Neuroplasticity subserving motor skill learning. Neuron. 2011;72(3):443–54. Available from: http://dx.doi.org/10.1016/j.neuron.2011.10.008
13. Berlot E, Popp NJ, Diedrichsen J. In search of the engram, 2017. Curr Opin Behav Sci. 2018;20.
14. Yokoi A, Diedrichsen J. Neural Organization of Hierarchical Motor Sequence Representations in the Human Neocortex. Neuron. 2019;103(6):1178–1190.e7.
15. Wymbs NF, Grafton ST. The human motor system supports sequence-specific representations over multiple training-dependent timescales. Cereb Cortex. 2015;25(11):4213–25.
16. Gross, C.G., Schiller, P.H., Wells, C., Gerstein GL. Single-unit activity in temporal association cortex of the monkey. J Neurophysiol. 1967;30(4):833–43.
17. Weiner KS, Sayres R, Vinberg J, Grill-Spector K. fMRI-adaptation and category selectivity in human ventral temporal cortex: Regional differences across time scales. J Neurophysiol. 2010;103(6):3349–65.
18. Grill-Spector K, Henson R, Martin A. Repetition and the brain: Neural models of stimulus-

specific effects. Trends Cogn Sci. 2006;10(1):14–23.
19. Grafton ST, Hamilton AFDC. Evidence for a distributed hierarchy of action representation in the brain. 2007;26:590–616.
20. Shmuelof L, Zohary E. Dissociation between Ventral and Dorsal fMRI. 2005;47:457–70.
21. Buckner RL, Goodman J, Burock M, Rotte M, Koutstaal W, Schacter D, et al. Functional-Anatomic Correlates of Object Priming in Humans Revealed by Rapid Presentation Event-Related fMRI. 1998;20:285–96.
22. Henson RN, Ganel T, Otten LJ. Electrophysiological and Haemodynamic Correlates of Face Perception , Recognition and Priming. 2003;793–805.
23. Noppeney U, Price CJ. An fMRI Study of Syntactic Adaptation. J Cogn Neurosci. 2004;16(4):702–13.
24. Barron HC, Vogels TP, Emir UE, Makin TR, O'Shea J, Clare S, et al. Unmasking Latent Inhibitory Connections in Human Cortex to Reveal Dormant Cortical Memories. Neuron. 2016;90(1):191–203. Available from: http://dx.doi.org/10.1016/j.neuron.2016.02.031
25. Alink A, Abdulrahman H, Henson RN. From neurons to voxels - repetition suppression is best modelled by local neural scaling. Nat Commun. 2018;9(3854):1–10. Available from: https://www.biorxiv.org/content/early/2017/07/31/170498
26. Diedrichsen J, Yokoi A, Arbuckle SA. Pattern component modeling: A flexible approach for understanding the representational structure of brain activity patterns. Neuroimage. 2017;
27. Barron HC, Garvert MM, Behrens TEJ. Repetition suppression: a means to index neural representations using BOLD? Philos Trans R Soc B Biol Sci. 2016;371(1705):20150355. Available from: http://rstb.royalsocietypublishing.org/lookup/doi/10.1098/rstb.2015.0355
28. Segaert K, Weber K, de Lange FP, Petersson KM, Hagoort P. The suppression of repetition enhancement: A review of fMRI studies. Neuropsychologia. 2013;51(1):59–66. Available from: http://dx.doi.org/10.1016/j.neuropsychologia.2012.11.006
29. Walther A, Ejaz N, Kriegeskorte N, Diedrichsen J. Representational fMRI analysis: an introductory tutorial. 2014;
30. Kriegeskorte N, Kievit RA. Representational geometry: Integrating cognition, computation, and the brain. Trends Cogn Sci. 2013;17(8):401–12.
31. Averbeck BB, Chafee M V, Crowe DA, Georgopoulos AP. Parallel processing of serial movements in prefrontal cortex. PNAS. 2002;99(20):13172–7.
32. Kornysheva K, Bush D, Meyer SS, Sadnicka A, Barnes G, Burgess N. Neural Competitive Queuing of Ordinal Structure Underlies Skilled Sequential Action. Neuron. 2019;101(6):1166–1180.e3.
33. Zimnik AJ, Churchland MM. Generation of Rapid Sequences by Motor Cortex. bioRxiv. 2020;
34. Picard N, Matsuzaka Y, Strick PL. Extended practice of a motor skill is associated with reduced metabolic activity in M1. Nat Neurosci. 2013;16(9):1340–7. Available from: http://www.pubmedcentral.nih.gov/articlerender.fcgi?artid=3757119&tool=pmcentrez&rendertype=abstract
35. Persichetti AS, Avery JA, Huber L, Merriam EP, Martin A. Layer-Specific Contributions to Imagined and Executed Hand Movements in Human Primary Motor Cortex. SSRN Electron J. 2019;1–5.
36. Summerfield C, Trittschuh EH, Monti JM, Mesulam MM, Egner T. Neural repetition suppression reflects fulfilled perceptual expectations. Nat Neurosci. 2008;11(9):1004–6.
37. Kok P, Jehee JFM, de Lange FP. Less Is More: Expectation Sharpens Representations in the Primary Visual Cortex. Neuron. 2012;75(2):265–70.
38. Garrido MI, Kilner JM, Kiebel SJ, Stephan KE, Friston KJ. Repetition suppression and plasticity in the human brain. Neuroimage. 2010;48(1):269–79.
39. James TW, Gauthier I. Repetition-Induced Changes in BOLD Response Reflect

Accumulation of Neural Activity. 2006;46:37–46.

40. Gotts SJ, Chow CC, Martin A. Repetition priming and repetition suppression : A case for enhanced efficiency through neural synchronization. Cogn Neurosci. 2012;3(May).
41. Ghuman AS, Bar M, Dobbins IG, Schnyer DM. The effects of priming on frontal-temporal communication. PNAS. 2008;105(24):8405–9.
42. Gilbert JR, Gotts SJ, Carver FW, Martin A. Object repetition leads to local increases in the temporal coordination of neural responses. Front Hum Neurosci. 2010;4(April):1–12.
43. Korzeniewska A, Wang Y, Benz HL, Fifer MS, Collard M, Milsap G, et al. Changes in human brain dynamics during behavioral priming and repetition suppression. Prog Neurobiol. 2020;189(May 2019).
44. Friston KJ, Worsley KJ, Poline J-PB, Frith CD, Frackowiak RSJ, Holmes a. P, et al. Statistical parametric maps in functional imaging: A general linear approach. Hum Brain Mapp. 1994;2(4):189–210. Available from: http://doi.wiley.com/10.1002/hbm.460020402
45. Dale AM, Fischl B, Sereno MI. Cortical Surface-Based Analysis. Neuroimage. 1999;9(2):179–94. Available from: http://www.ncbi.nlm.nih.gov/pubmed/9931268%0Ahttp://linkinghub.elsevier.com/retrieve/pii/S1053811998903950
46. Fischl B, Rajendran N, Busa E, Augustinack J, Hinds O, Yeo BTT, et al. Cortical folding patterns and predicting cytoarchitecture. Cereb Cortex. 2008;18(8):1973–80.
47. Yousry TA, Schmid UD, Alkadhi H, Schmidt D, Peraud A, Buettner A, et al. Localization of the motor hand area to a knob on the precentral gyrus. A new landmark. Brain. 1997;120(1):141–57.
48. Walther A, Nili H, Ejaz N, Alink A, Kriegeskorte N, Diedrichsen J. Reliability of dissimilarity measures for multi-voxel pattern analysis. Neuroimage. 2016;137:188–200. Available from: http://dx.doi.org/10.1016/j.neuroimage.2015.12.012
49. Oosterhof NN, Wiestler T, Downing PE, Diedrichsen J. A comparison of volume-based and surface-based multi-voxel pattern analysis. Neuroimage. 2011;56(2):593–600. Available from: http://dx.doi.org/10.1016/j.neuroimage.2010.04.270
50. Diedrichsen J, Provost S, Zareamoghaddam H. On the distribution of cross-validated Mahalanobis distances. arXiv Prepr arXiv. 2016;1607.01371. Available from: http://arxiv.org/abs/1607.01371
51. Diedrichsen J, Ridgway GR, Friston KJ, Wiestler T. Comparing the similarity and spatial structure of neural representations: A pattern-component model. Neuroimage. 2011;55(4):1665–78. Available from: http://dx.doi.org/10.1016/j.neuroimage.2011.01.044
52. Ejaz N, Hamada M, Diedrichsen J ouml rn. Hand use predicts the structure of representations in sensorimotor cortex. Nat Neurosci. 2015;18(7):1034–40. Available from: http://dx.doi.org/10.1038/nn.4038%5Cnpapers3://publication/doi/10.1038/nn.4038
53. Nili H, Wingfield C, Walther A, Su L, Marslen-Wilson W, Kriegeskorte N. A Toolbox for Representational Similarity Analysis. PLoS Comput Biol. 2014;10(4):e1003553.